ELSEVIER

European Journal of Pharmacology 361 (1998) 157–163

ejp

σ-Binding site ligands inhibit K^+ currents in rat locus coeruleus neurons in vitro

Vu H. Nguyen [a,c], Susan L. Ingram [a], Michael Kassiou [d], MacDonald J. Christie [a,b,*]

[a] *Department of Pharmacology D06, The University of Sydney, Sydney, NSW 2006, Australia*
[b] *The Medical Foundation, The University of Sydney, Sydney, NSW 2006, Australia*
[c] *Radiopharmaceuticals R&D Division, ANSTO, NSW 2234, Australia*
[d] *PET Department, Royal Prince Alfred Hospital, NSW 2050, Australia*

Received 2 July 1998; revised 23 September 1998; accepted 25 September 1998

Abstract

Biological actions of novel σ_1- and σ_2-selective binding site ligands (trishomocubanes: 4-azahexacyclo [5.4.1.0.^{2,6}.0^{3,10}.0^{5,9}.-0^{8,11}]dodecanes), and the reference ligands, 1,3-di(2-tolyl)-guanidine (DTG), haloperidol, (+)-pentazocine and dextromethorphan, were studied in rat locus coeruleus neurons using intracellular and whole-cell patch clamp recordings. High concentrations of trishomocubanes produced small inward currents and affected some parameters of action potential waveforms suggesting modest potency to inhibit ionic conductances underlying action potentials. σ-Ligands produced large inward currents in the presence of μ-opioid, α_2-adrenoceptor and ORL1 receptor agonists. These reversed polarity near the K^+ equilibrium potential, suggesting that σ-ligands act as ligand activated K^+-channel blockers or interfere with the coupling between these receptors and K^+-channels. However, no correlation was found between binding affinities at σ_1- or σ_2-binding sites and potency to inhibit K^+-currents, suggesting that these effects on K^+-channels are not directly related to occupancy of σ binding sites.

Keywords: σ Receptor; Trishomocubane; Nociceptin; Opioid; Locus coeruleus; K^+ channel

1. Introduction

Although putative σ-receptor ligands have been shown to exhibit a variety of effects on the central nervous system, their cellular electrophysiological actions have not been thoroughly characterised (e.g., Su, 1993). Various σ-ligands have been reported to modify K^+-conductances in several different tissues (Bobker et al., 1989; Kennedy and Henderson, 1990; JeanJean et al., 1993; Kobayashi et al., 1997), suggesting that σ-receptors may be associated with K^+-channels. Wu et al. (1991) and Morio et al. (1994) independently reported that σ-receptor ligands blocked a tonic K^+-conductance with a rank order of potency suggestive of an interaction with σ_2-binding sites. However, the concentrations of σ-ligands producing these effects were somewhat higher than their affinities at σ_2-binding sites.

Rat locus coeruleus neurons have been shown to possess a relatively high density of σ binding sites (Weber et al., 1986). These cells also express a number of receptors that increase an inwardly rectifying K^+-conductance, including μ-opioid (North and Williams, 1985), α_2-adrenoceptors (North and Williams, 1985) and ORL1 receptors (Connor et al., 1996). Some biological actions of σ-ligands have been reported in the locus coeruleus (Elam et al., 1986; Bobker et al., 1989). Bobker et al. (1989) demonstrated that σ-ligands including 1,3-di(2-tolyl)-guanidine (DTG) and (+)-3-(3-hydroxyphenyl)-*N*-(1-propyl)piperidine [(+)-3-PPP] excited locus coeruleus neurons and inhibited ligand-induced hyperpolarizations caused by μ-opioid receptors and α_2-adrenoceptors. They suggested that this action could be due to interaction with either K^+-channels or second messenger systems but were unable to identify whether or not the effects were caused by specific interaction with by σ-binding sites due to lack of availability of high-affinity and subtype selective σ-ligands. The purpose of the present study was to investigate the electrophysiological effects of novel, σ-selective-ligands (trishomocubanes; Nguyen et al., 1996) having a range of affinity and selectivity for σ_1- and σ_2-binding sites.

* Corresponding author. Tel.: +61-2-9351-2295; Fax: +61-2-9351-3868; E-mail: macc@pharmacol.su.oz.au

0014-2999/98/$ - see front matter
PII: S0014-2999(98)00706-7

2. Materials and methods

2.1. Materials

Trishomocubanes, 4-azahexacyclo[5.4.1.$0^{2,6}$.$0^{3,10}$.$0^{5,9}$.$0^{3,8}$]dodecanes (ANSTO-6,7,10,13,14,16-19), were synthesised at the Australian Nuclear Science and Technology Organisation, Radiopharmaceuticals R & D Division (Menai, NSW, Australia) as previously described (Kassiou et al., 1996; Nguyen et al., 1996). UK 14304 (5-Bromo-*N*-(4,5-dihydro-1*H*-imidazol-2-yl)-6 quinoxalinamine), (+)-Pentazocine, DTG, dextromethorphan hydrobromide, idazoxan hydrochloride, and prazosin hydrochloride were purchased from Research Biochemicals (Natick, MA, USA). Haloperidol and met-enkephalin were from Sigma (St. Louis, MO, USA). Nociceptin (Orphinin FQ; Phe-Gly-Gly-Phe-Thr-Gly-Ala-Arg-Lys-Ser-Ala-Arg-Lys-Leu-Ala-Asn-Gln) was synthesised and purified by Chiron Mimotopes (Clayton, Victoria, Australia). Buffer salts were from BDH Australia. Stock solutions of trishomocubanes and DTG were dissolved in DMSO (Dimethyl Sulphoxide); other chemicals were made up in distilled water. Haloperidol and (+)-pentazocine were dissolved in distilled water with the help of 1–2 drops of glacial acetic acid. Stock solutions of drugs were diluted to working concentrations by using the physiological saline solution and applied by superfusion.

2.2. Slice preparation and electrophysiological recordings

Male Sprague–Dawley rats (150–200 g, 5–7 weeks old) were anaesthetised with halothane and killed by cervical dislocation and tissue slices containing locus coeruleus prepared as previously described (Connor et al., 1996). The content of the physiological saline solution was (in mM) 126 NaCl, 2.5 KCl, 1.2 NaH_2PO_4, 1.2 $MgCl_2$, 2.4 $CaCl_2$, 11 glucose, and 24 $NaHCO_3$ and was saturated with 95% O_2/5% CO_2. Drugs were applied to the slice by changing the solution to one that differed only in its content of the drug. Membrane potential and current was recorded with microelectrodes (35–70 MΩ, filled with 2 M KCl) using a single electrode current- and voltage-clamp (Axoclamp-2A, Axon Instruments, Foster City, CA), or in some experiments (as noted in text), using whole cell patch clamp recording (Axopatch 1D) with electrodes (2–4 MΩ) filled with internal solution composed of (mM): K-gluconate 125, NaCl 15, $MgCl_2$ 2, HEPES 10, EGTA 11, MgATP 1, NaGTP 0.25, pH 7.3. Recordings were made as described elsewhere (Connor et al., 1997; Osoborne et al., 1996).

2.3. [^{3}H](+)-pentazocine and [^{3}H]DTG receptor binding assays

The binding assay was performed essentially as described by Nguyen et al. (1996), except the assay buffer was the physiological saline containing HEPES solution with a composition (in mM) of: 126 NaCl, 2.5 KCl, 1.2 NaH_2PO_4, 1.2 $MgCl_2$, 2.4 $CaCl_2$, 11 glucose, 24 $NaHCO_3$, and 22 HEPES, adjusted to pH 7.4 (at room temperature) with NaOH.

2.4. Data analysis

All data are expressed as mean ± S.E.M. Statistical significance was determined using paired, two-tailed *t*-test at $P < 0.05$. Correlations between binding affinity at σ-binding sites and potency of K^+-current inhibition by σ-ligands were performed using both Pearson product-moment correlation (r_p) and the Spearman rank correlation coefficients (r_S).

Table 1
Effects of ANSTO-14 and ANSTO-19 on membrane properties of locus coeruleus neurons

Treatment	Action potential			After-hyperpolarization	
	Peak (mV)	Rise (ms)	Halfwidth (ms)	A-H Peak (mV)	A-H Halfwidth (ms)
Control	80.8 ± 1.9	0.52 ± 0.08	0.72 ± 0.04	−19.0 ± 0.5	−46.9 ± 5.6
ANSTO-14 (% control)					
1 μM	102.6 ± 6.2	70.0 ± 10.2	89.0 ± 12.8	98.7 ± 5.3	112.2 ± 38.5
3 μM	99.2 ± 5.8	93.4 ± 3.8[a]	91.0 ± 6.6	92.6 ± 4.9	158.2 ± 45.3
10 μM	102.0 ± 2.4	105.8 ± 22.3	89.3 ± 5.8	94.0 ± 3.3	146.4 ± 21.6[a]
30 μM	85.8 ± 7.2	126.9 ± 15.3	149.4 ± 21.7	78.6 ± 2.9[a]	174.4 ± 18.1[a]
ANSTO-19 (% control)					
1 μM	98.0 ± 2.6	108.5 ± 10.0	103.9 ± 5.5	96.4 ± 1.6	80.7 ± 27.4
3 μM	99.7 ± 2.5	106.5 ± 12.3	96.0 ± 1.8	91.6 ± 2.5	131.0 ± 43.7
10 μM	97.6 ± 2.7	115.0 ± 18.6	100.2 ± 3.1	89.2 ± 3.2	152.4 ± 51.0
30 μM	92.1 ± 4.4[a]	122.5 ± 5.6[a]	120.1 ± 9.6[a]	82.5 ± 2.7[a]	110.9 ± 44.3

Data from drug treatments are presented as mean ± S.E.M.% of pre-drug control, $n = 3$–5 single cells.
Data from controls are presented as means ± S.E.M., $n = 16$ single cells for each parameter.
[a] Denotes for $P < 0.05$ using paired, two-tailed *t*-test.

3. Results

3.1. General membrane properties

ANSTO-14 and ANSTO-19 were tested for their effects on the membrane properties including the action potential waveform and the intrinsic firing rate. Sufficient constant current was applied to neurons throughout the experiment to fire action potentials spontaneously at frequencies of 1–3 Hz, which is similar to their behaviour in vivo (Korf et al., 1974). ANSTO-19 at concentrations of less than 30 μM had no effect on firing rate or action potential waveform. ANSTO-14 (10 μM) increased both the duration (measured at 50% peak height) of the after-hyperpolarization (A-H) peaks and decreased the amplitude of the after-hyperpolarization (A-H) peaks (Table 1). ANSTO-19 at 30 μM decreased both the amplitudes of both the action potentials and the A-H peaks, respectively. However, ANSTO-19 increased the duration of the action potential (Table 1).

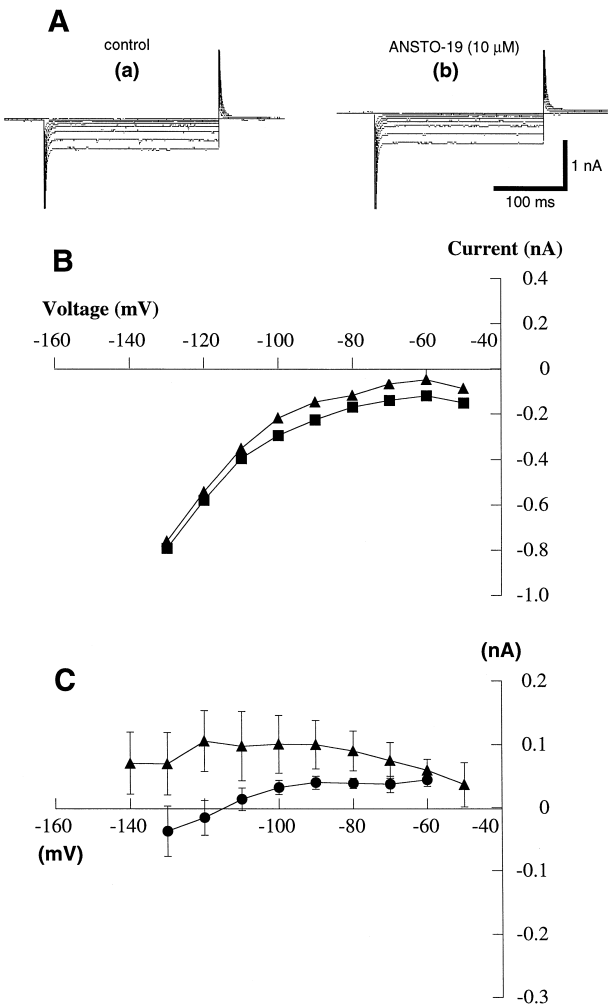

Fig. 1. σ-ligands inhibit background K^+ currents in locus coeruleus neurons. Recordings were made by the whole-cell patch-clamp technique, as outlined in Section 2. Panel A: Voltage command steps 250 ms in duration were made in 10 mV increments from −50 to −140 mV from a holding potential of −60 mV. Representative raw traces of currents in the absence (Control, **a**) and presence of ANSTO-19 (10 μM, **b**) in a single neuron are shown. Panel B: The current-voltage relationship from the same neuron (control ▲, ANSTO-19 ■,) is plotted from the mean amplitudes of evoked currents shown in panel A. Panel C: Current–voltage relationships ($n = 6–7$ neurons at each point) of the current inhibited by ANSTO-19 (●) and DTG (▲) (control current subtracted from current in the presence of the σ-ligand).

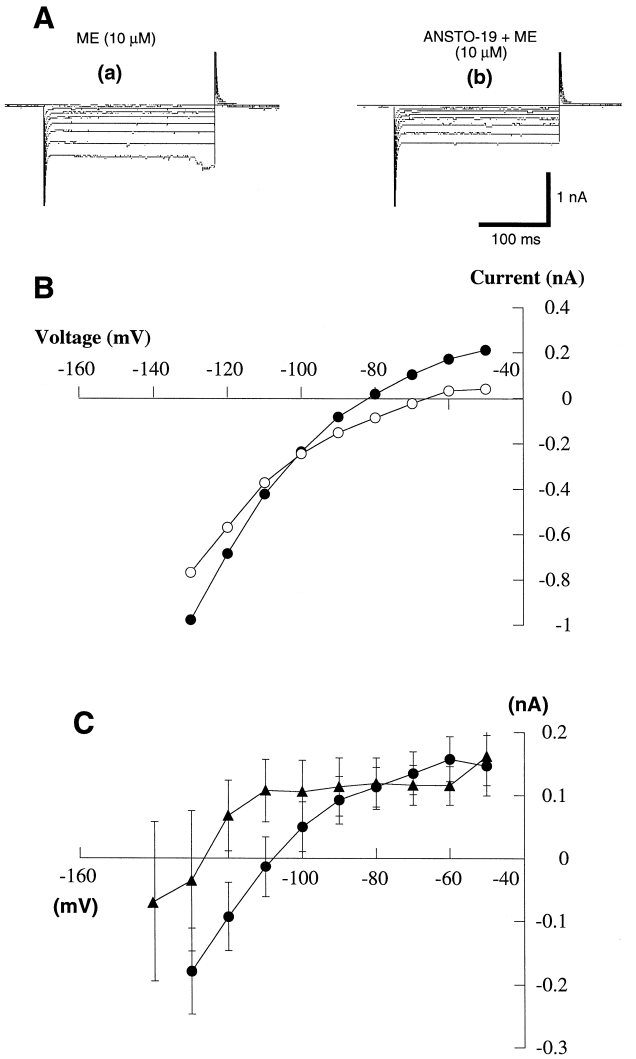

Fig. 2. σ-Ligands inhibit met-enkephalin-activated K^+ currents in locus coeruleus neurons. Panel A: Representative raw traces of the met-enkephalin-activated currents in the absence (Control, **a**) and presence of ANSTO-19 (10 μM, **b**) in a single neuron (same neuron and voltage clamp protocol as in Fig. 1). Panel B: The steady-state current–voltage relationship from the same neuron in met-enkephalin, (●), and in ANSTO-19 in the presence of met-enkephalin (○) is plotted from the mean amplitudes of currents shown in Panel A. Panel C: Current–voltage relationships ($n = 6–7$ neurons at each point) of the met-enkephalin activated current inhibited by ANSTO-19 (●) and DTG (▲) (current in the presence of met-enkephalin subtracted from current in the presence of the σ-ligand plus met-enkephalin).

3.2. Inhibition of background inwardly rectifying K^+-currents

The effects of ANSTO-19 and DTG (both 10 μM) on steady state current–voltage relationships were examined using whole-cell patch-clamp recordings using coronal locus coeruleus slices to optimise voltage control of the neurons (see Travagli et al., 1996). The resting membrane conductance measured between −60 and −90 mV was 4.1 ± 0.4 nS ($n = 13$) and at potentials between −110 and −130 mV was 16.2 ± 1.1 nS ($n = 12$). ANSTO-19 (Fig. 1) and DTG both produced significant inward currents at −60 mV. ($P = 0.007$, paired $t = 4.42$, $n = 6$ and $P = 0.02$, paired $t = 3.1$, $n = 7$ for ANSTO-19 and DTG, respectively), although the amplitude was rather small. Current–voltage relationships of the current presumably inhibited by these ligands were determined by subtraction. Fig. 1C shows pooled current–voltage relationships of the control minus ANSTO-19 or DTG induced currents (i.e., the current presumably blocked by these ligands). Where a reversal potential could be determined it was −100 ± 4 mV for ANSTO-19 ($n = 2$ out of 6 cells), however it could not be determined for DTG ($n = 0$ out 7 cells).

3.3. Inhibition of met-enkephalin activated K^+-currents

Met-enkephalin (10 μM) increased membrane conductance to 6.8 ± 0.7 nS ($n = 13$) between −60 and −90 mV, and 20.6 ± 2.1 nS at between −110 and −130 mV ($n = 12$). ANSTO-19 reduced conductances significantly from 7.7 ± 1.4 nS to 4.7 ± 0.8 nS (at potential of −60 mV, $P = 0.02$, paired $t = 3.3$, df 5) and from 27.0 ± 2.6 nS to 17.3 ± 1.5 nS (at potential of −120 mV, $P = 0.01$, paired $t = 4.5$, df 5) (Fig. 2B,C). Representative raw traces of evoked currents and steady-state current–voltage plots of ANSTO-19-induced inhibition of met-enkephalin-activated K^+-currents are presented in Fig. 2A and B, respectively. The pooled met-enkephalin-induced currents

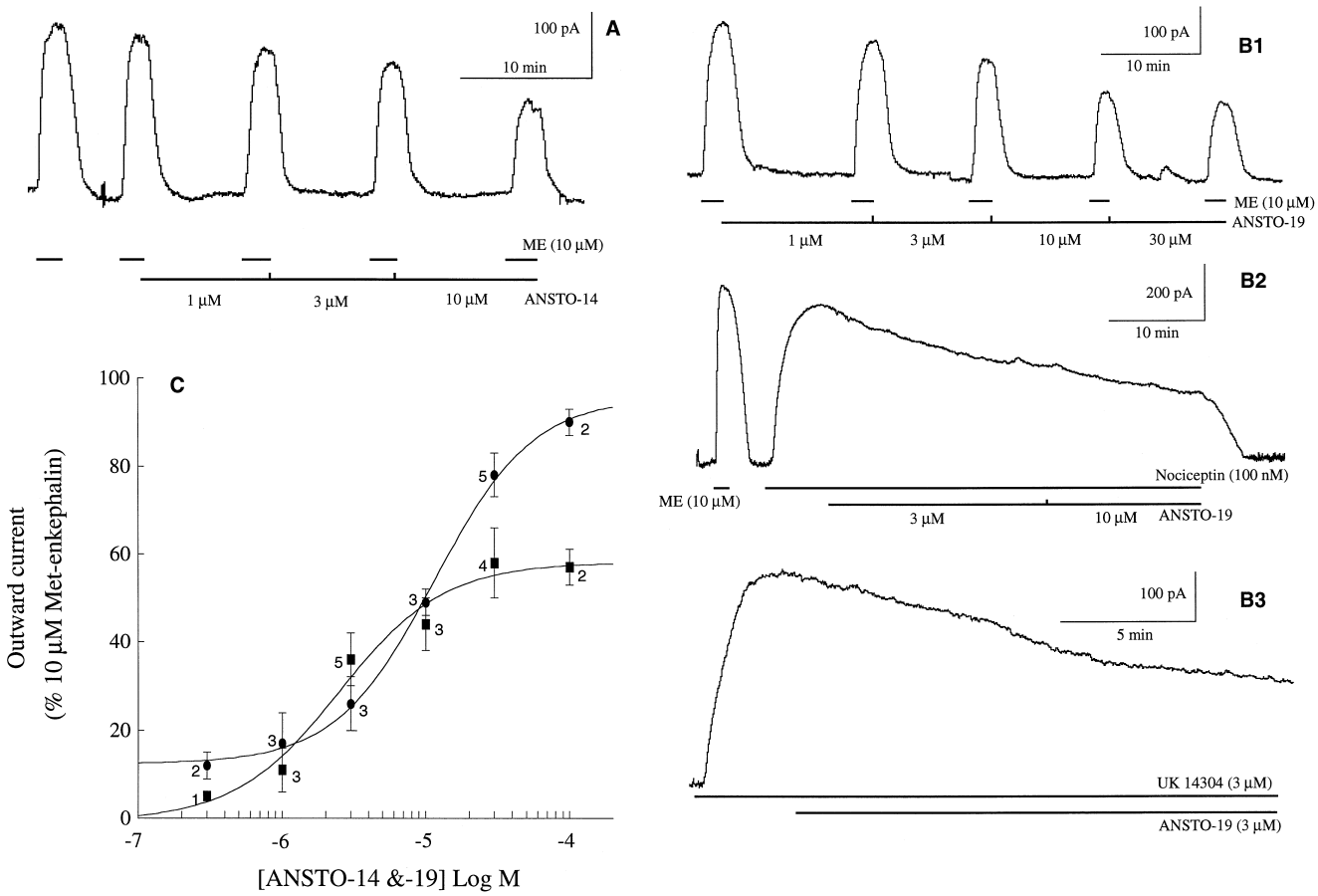

Fig. 3. The potency of trishomocubanes, ANSTO-14 and ANSTO-19 on ligand-induced K^+ currents in locus coeruleus neurons. Cells were voltage-clamped at a potential of −60 mV and drugs were superfused for the duration shown by the horizontal bars. Panel A: Membrane currents induced by met-enkephalin (10 μM) and increasing concentrations of ANSTO-14 (100 nM-300 μM) in a single neuron. Panel B: Examples of membrane currents induced by met-enkephalin (10 μM), nociceptin (100 nM) and UK 14304 (3 μM), respectively and increasing concentrations of ANSTO-19 (1–10 μM) in single locus coeruleus neurons. Panel C: Concentration–response relationships of inhibition of met-enkephalin-induced K^+-currents produced by ANSTO-14 (●) and ANSTO-19 (■). Each point represents between 4–5 individual cells tested at each concentration of the ligand, with the number of cells indicated above the point. The points were fitted with a logistic function yielding the IC_{50}s of 11.5 ± 1.2 and 2.5 ± 0.6 μM for ANSTO-14 and ANSTO-19, respectively.

Table 2
IC_{30} values and corresponding rankings of selected σ ligands in inhibition of met-enkephalin-induced K^+-currents, σ_1- and σ_2-binding in locus coeruleus neurons

Drug	K^+-current inhibition pIC_{30} (rank)	Low salt pIC_{50} σ_1 (rank)	Physiol. pIC_{50} σ_1 (rank)	Low salt pIC_{50} σ_2 (rank)	Physiol. pIC_{50} σ_2 (rank)
ANSTO-6	5.04 (10)	6.79 (8)	ND	7.25 (5)	ND
ANSTO-7	5.22 (7)	6.48 (12)	6.5 (6)	7.35 (4)	7.21 (1)
ANSTO-10	5.14 (9)	7.50 (5)	ND	6.47 (11)	ND
ANSTO-13	5.19 (8)	7.48 (6)	7.21 (3)	6.58 (10)	7.02 (4)
ANSTO-14	5.30 (4)	7.84 (3)	7.36 (2)	6.72 (9)	7.01 (5)
ANSTO-16	5.23 (6)	6.81 (7)	6.66 (5)	6.92 (8)	7.05 (3)
ANSTO-17	5.25 (5)	6.57 (10)	ND	7.22 (6)	ND
ANSTO-18	5.49 (2)	6.53 (11)	6.44 (7)	7.48 (3)	7.18 (2)
ANSTO-19	5.89 (1)	6.62 (9)	6.42 (8)	7.65 (2)	6.94 (6)
DTG	4.84 (11)	7.57 (4)	6.75 (4)	7.00 (7)	6.75 (7)
(+)-Pentazocine	5.40 (3)	8.27 (2)	8.57 (1)	ND	5.52 (8)
Dextromethorphan	4.40 (12)	6.37 (13)	6.28 (9)	4.04 (12)	4.74 (9)
Haloperidol	< 4.40 (13)	8.69 (1)	ND	7.83 (1)	ND

K^+-current (induced by met-enkephalin) inhibition data are presented as mean IC_{30} from 3–7 single neurons along with their corresponding potency rankings. IC_{50} values and corresponding ranking of σ-ligands to inhibit [^{3}H](+)-pentazocine (σ_1) and [^{3}H]DTG (σ_2) binding under optimized binding conditions (Low salt) as reported in Nguyen et al. (1996), or in physiological saline/HEPES buffer, pH 7.4 (Physiol.) as described in Section 2.

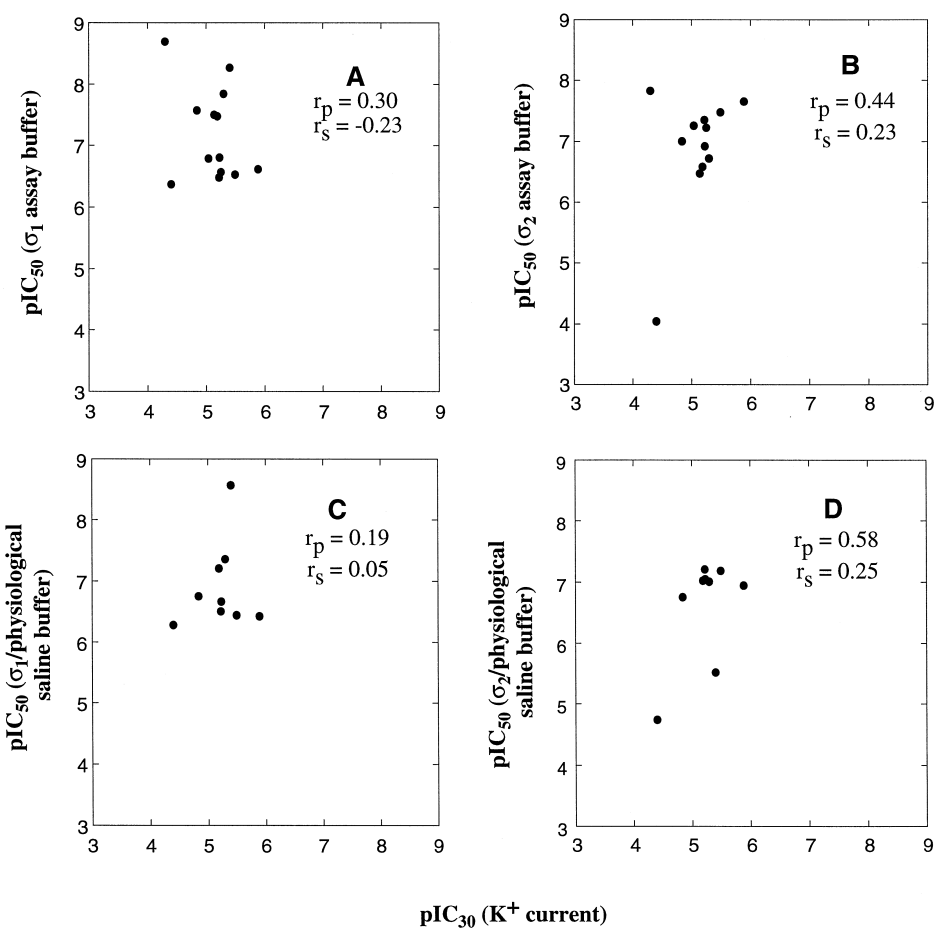

Fig. 4. Scatter plots of the potencies of inhibition of met-enkephalin induced K^+ currents (pIC_{30}s) by trishomocubanes and other σ-ligands against their corresponding binding potency (pIC_{50}s) at σ_1 (Panel A), and at σ_2 binding sites (Panel B) in the optimized σ_1/σ_2 binding assay buffers, and in the physiological saline/HEPES buffer, pH 7.4 (σ_1, Panel C; σ_2, Panel D). Inset values show Pearson product moment correlations of pIC_{30}s vs. pIC_{50}s (r_P) and Spearman's rank order correlation of their ranks (r_S) for each binding assay condition.

inhibited by ANSTO-19 (current in the presence of met-enkephalin minus met-enkephalin plus test drug) are plotted in Fig. 2C. DTG also inhibited met-enkephalin-induced K^+-currents (Fig. 2C). The reduction in conductance produced by DTG was not significantly different from control at -60 mV (from 6.0 ± 0.5 nS to 6.1 ± 0.3 nS) but was significant at -130 mV (from 16.0 ± 1.4 nS to 12.5 ± 1.8 nS, $P < 0.01$, paired $t = 3.6$, df 6).

3.4. Potency of inhibition of ligand-activated K^+-currents

A concentration near the peak of the met-enkephalin concentration–response curve (10 μM) was chosen as the test dosage (Bobker et al., 1989) to establish inhibitory potencies of σ-ligands. Two sequential met-enkephalin applications were performed before applying test drugs to ensure a reproducible effect of met-enkephalin was present. Both ANSTO-14 and ANSTO-19 were tested for their effects against met-enkephalin (10 μM)-induced K^+-currents in a concentration range of (0.3–100 μM). The maximal inhibition of met-enkephalin induced K^+-currents was $83 \pm 5\%$ for ANSTO-14, but only $58 \pm 4\%$ for ANSTO-19, yielding IC_{50} values of 11.5 ± 1.2 and 2.5 ± 0.6 μM, respectively (Fig. 3, Panel C). Neither drug produced a complete inhibition of the met-enkephalin-induced K^+-currents at the concentrations tested, nor washed out for up to 45 min. Fig. 3 shows representative raw traces of the effects of ANSTO-14 (Panel A) and ANSTO-19 (Panel B1) on met-enkephalin-induced K^+-currents and their concentration–response curves (Panel C).

All trishomocubanes (3–30 μM) and reference σ-ligands including (+)-pentazocine, DTG, haloperidol, and dextromethorphan (3–100 μM) inhibited met-enkephalin-induced K^+-currents. IC_{30} values of the various ligands are presented in Table 2. The IC_{30} was used instead of the IC_{50} because many of these compounds still failed to inhibit sufficiently to determine IC_{50} values at high concentrations.

UK 14304 and nociceptin (orphanin FQ) activate the same K^+-conductance as met-enkephalin in locus coeruleus neurons (e.g., Connor et al., 1996). ANSTO-14 (10 μM) and ANSTO-19 (3 μM), produced $44.3 \pm 2.4\%$ ($n = 6$) and $44.2 \pm 3.3\%$ ($n = 7$) of the inhibition of the UK 14304-induced K^+-currents (Fig. 4 B2 and B3). The inhibition of nociceptin-induced K^+-currents by ANSTO-14 and ANSTO-19 were dose-dependent with estimated IC_{50} values of 4.1 ± 0.4 ($n = 4$) and 9.3 ± 2.0 μM ($n = 5$), respectively.

3.5. Correlation between inhibition of ligand-activated K^+-currents and σ-binding potency

The relationship between potencies of trishomocubanes and selected σ-ligands to inhibit K^+-currents and σ_1- or σ_2-binding was examined. Data for inhibition of σ-binding was taken from our previous study (Nguyen et al., 1996) and was also characterised using a physiological saline/HEPES (pH 7.4) buffer in order to correlate binding affinity with potency to inhibit K^+-currents under the same ionic conditions. Data from these binding studies are also presented in Table 2.

No significant correlations were found between the potencies to inhibit met-enkephalin-induced K^+-currents by these σ-ligands and the binding affinity at either σ_1- or σ_2-binding sites, in both the usual σ_1- and σ_2-binding assay buffers (Nguyen et al., 1996) and the physiological saline/HEPES buffer (Fig. 4). In most cases binding IC_{50}s were approximately two orders of magnitude smaller than IC_{30}s for K^+-current inhibition.

4. Discussion

High concentrations of both ANSTO-14 and ANSTO-19 were able to affect some parameters of the action potential waveform such as amplitude and duration of both the action potential and the after-hyperpolarization. These findings indicate that high concentrations of trishomocubanes may interfere with channels that are permeable to Ca^{2+} (changes in duration of action potential), Na^+ (changes in amplitude of action potential), and K^+ (changes in duration of action potential and after-hyperpolarization) but the relationship between such observations and occupancy of σ-binding sites is not established.

Inhibition of the background K^+-currents was small (usually less than 50 pA at -60 mV) and not easily quantified. Nonetheless the inward current produced by ANSTO-19 in the absence of receptor stimulation reversed polarity near the expected K^+ equilibrium potential suggesting inhibition of the background K^+-conductance (Williams et al., 1988). It is not clear whether DTG inhibited this conductance because a reversal potential was not observed in any cells. The failure to observe a reversal potential in some cells was most likely due to the small amplitude of the inward currents and poor voltage clamp control of dendrites (Travagli et al., 1996).

Many of the σ-ligands tested produced substantial inhibition of ligand activated K^+-currents. Inward currents produced by ANSTO-19 and DTG in the presence of met-enkephalin showed inward rectification and often reversed polarity near the predicted K^+ equilibrium potential (-104 mV). Furthermore, ANSTO-14 and ANSTO-19 also inhibited met-enkephalin, nociceptin and UK 14304-induced K^+-currents with similar potency. This suggests that trishomocubanes block the common pathway between μ-opioid, nociceptin and α_2-adrenoceptors, and K^+-channels. This is similar to the interpretation of Bobker et al. (1989), that σ-ligands block ligand-activated inwardly rectifying K^+-channels but contrary to the suggestion that σ-ligands are nociceptin (ORL1) receptor antagonists on the basis of similar results reported for σ-ligand inhibition of nociceptin activated inwardly rectifying K^+-channel expressed in Xenopus oocytes (Kobayashi et al., 1997).

Previous radioligand binding studies showed that ANSTO-14 and ANSTO-19 have high affinity and selectivity for σ_1- and σ_2-binding sites (K_is = 9.4 and 19 nM), respectively (Nguyen et al., 1996). These experiments were repeated in physiological saline solution in the present study. The IC_{50}s of some of these ligands differed somewhat under physiological conditions. This could have been due to changes in ionic strengths of the buffers or divalent cations (Rothman et al., 1991). An effect of pH may also have contributed to this shift because both σ_1-([^{3}H](+)-pentazocine) and σ_2- ([^{3}H]DTG) binding were optimal at higher pHs (i.e., > 8.0, data not shown).

All trishomocubanes and reference compounds tested had inhibitory effects on met-enkephalin-activated K^+-currents. Despite the fact that many of the drugs studied here have very high affinity for σ-binding sites, especially haloperidol and (+)-pentazocine, potency to inhibit ligand activated K^+-currents was consistently in the micromolar range. Furthermore, no significant correlation between inhibition of met-enkephalin-induced K^+-currents and potency of binding to σ-sites was observed, under either usual (Nguyen et al., 1996) or physiological binding conditions. We therefore conclude that the inhibitory effects of trishomocubanes and other σ reference compounds described here are not related directly to their interactions with σ_1- or σ_2-binding sites. The K^+-channel blocking action must therefore be due to physicochemical properties weakly related to their interactions with σ-binding sites.

Acknowledgements

Supported by the National Health and Medical Research Council of Australia. S.L. Ingram was supported by a Human Frontier Science Fellowship and MJ Christie by the Medical Foundation of The University of Sydney.

References

Bobker, D.H., Shen, K.-Z., Surprenant, A., Williams, J.T., 1989. DTG and (+)-3-PPP inhibit a ligand-activated hyperpolarization in mammalian neurons. J. Pharmacol. Exp. Ther. 251, 840–845.

Connor, M., Ingram, S.L., Christie, M.J., 1997. Cortistatin increase of a potassium conductance in rat locus coeruleus neurons in vitro. Brit. J. Pharmacol. 122, 1567–1572.

Connor, M., Vaughan, C.W., Chieng, B., Christie, M.J., 1996. Nociceptin receptor coupling to a potassium conductance in rat locus coeruleus neurons in vitro. Br. J. Pharmacol. 119, 1614–1618.

Elam, M., Clark, D., Svensson, T.H., 1986. Electrophysiological effects of the enantiomers of 3-PPP on neurons in the locus coeruleus of the rat. Neuropharmacol. 25, 1003–1008.

JeanJean, A.P., Mestre, M., Maloteaux, J.-M., Laduron, P.M., 1993. Is the σ_2 receptor in rat brain related to the K channel of class III antiarrhythmic drugs?. Eur. J. Pharmacol. 241, 111–116.

Kassiou, M., Nguyen, V.H., Knott, R., Christie, M.J., Hambley, T.W., 1996. Trishomocubanes, a new class of selective and high affinity ligands for the sigma binding sites. Bioorg. Med. Chem Lett. 6, 595.

Kennedy, C., Henderson, G., 1990. Inhibition of potassium currents by the sigma receptor ligand (+)-3-(3-hydroxyphenyl)-*N*-(1-propyl)piperidine in sympathetic neurons of the mouse isolated hypogastric ganglion. Neuroscience 35, 725–733.

Kobayashi, T., Ikeda, K., Togashi, S., Itoh, N., Kumanishi, T., 1997. Effects of sigma ligands on the nociceptin/orphanin FQ receptor co-expressed with the G-protein-activated K^+ channel in Xenopus oocytes. Br. J. Pharmacol. 120, 986–987.

Korf, J., Bunney, B.S., Aghajanian, G.K., 1974. Noradrenergic neurons: morphine inhibition of spontaneous activity. Eur. J. Pharmacol. 25, 165–169.

Morio, Y., Tanimoto, H., Yakushiji, T., Moromoto, Y., 1994. Characterization of currents induced by sigma ligands in NCB20 neuroblastoma cells. Brain Res. 637, 190–196.

Nguyen, V.H., Kassiou, M., Johnston, G.A.R., Christie, M.J., 1996. Comparison of binding parameters of σ_1 and σ_2 binding sites in rat and guinea pig brain membraines: Novel subtype-selective trishomocubanes. Eur. J. Pharmacol. 311, 233–240.

North, R.A., Williams, J.T., 1985. On the potassium conductance increased by opioids in rat locus coeruleus neurons. J. Physiol. (Lond.) 364, 265–280.

Osoborne, P.B., Vaughan, C.W., Wilson, H.I., Christie, M.J., 1996. Opioid inhibition of rat periaqueductal grey neurons with identified projections to rostral ventralmedial medulla in vitro. J. Physiol. (Lond.) 490, 383–389.

Rothman, R.B., Reid, A., Mahdoubia, A., Kim, C.-H., DeCosta, B.R., Jacobson, A.E., Rice, K.C., 1991. Labeling by [^{3}H]1,3-Di(2-tolyl)guanidine of two high affinity binding sites in guinea pig brain: evidence for allosteric regulation by calcium channel antagonists and pseudoallosteric modulation by σ ligands. Mol. Pharmacol. 39, 222–232.

Su, T.P., 1993. Delineating biochemical and functional properties of sigma receptors: emerging concepts. Crit. Rev. Neurobiol. 7, 187–203.

Travagli, R.A., Wessendorf, M., Williams, J.T., 1996. Dendritic arbor of locus coeruleus neurons contributes to opioid inhibition. J. Neurophysiol. 75, 2029–2035.

Weber, E., Sonders, M., Quaram, M., McLean, S., Pou, S., Keana, J.F.W., 1986. 1,3-Di(2-[5−^{3}H]tolyl)guanidine: A selective ligand that labels σ-type receptors for psychotomimetic opiates and antipsychotic drugs. Proc. Natl. Acad. Sci. U.S.A. 83, 8784–8788.

Williams, J.T., North, R.A., Tokimasa, T., 1988. Inward rectification of background and opiate-activated potassium currents in rat locus coeruleus neurons. J. Neurosci. 8, 4299–4306.

Wu, X.-Z., Bell, J.A., Spivak, C.E., London, E.D., Su, T.-S., 1991. Electrophysiological and binding studies on intact NCB-20 cells suggest presence of a low affinity sigma receptor. J. Pharmacol. Exp. Ther. 257, 351–359.